JOURNAL OF EXPERIMENTAL AND THEORETICAL PHYSICS, 2024, Vol. 165, No. 6, pp. 851–858

ELECTRONIC PROPERTIES OF SOLID

CAPTURE OF ELECTRONS AND HOLES ON MERCURY VACANCIES VIA SINGLE OPTICAL PHONON EMISSION DURING SHOCKLEY–READ–HALL RECOMBINATION IN A NARROW GAP HGCDTE

© 2024 D. V. Kozlov[a, b], V. V. Rumyantsev[a, b], A. A. Yantser[a, b*], S. V. Morozov[a, b], V. I. Gavrilenko[a, b]

[a] *Institute for Physics of Microstructures, Russian Academy of Sciences; 603087, Nizhniy Novgorod, Russia*

[b] *Lobachevsky Nizhny Novgorod State University 603950, Nizhny Novgorod, Russia*

** e-mail: yantser@ipmras.ru*

Received November 06, 2023

Revised January 16, 2024

Accepted January 18, 2024

Abstract. The aim of the present work is to calculate the recombination time of Shockley–Read–Hall (SRH) process with the capture of charge carriers on mercury vacancy states in HgCdTe ternary alloys with a bandgap of about 40 meV. In the considered case the capture of both electron and hole is possible due to the emission of a single optical phonon. It is found that at T = 4.2 K and T = 77 K the SRH recombination determines the total lifetime of carriers in the p-type material with recombination centers density more than ~$2 \cdot 10^{15}$ cm^{-3}, which makes it possible to control the lifetime of carriers by changing the concentration of mercury vacancies.

Keywords: *HgCdTe, Shockley-Read-Hall recombination, mercury vacancy*

DOI: 10.31857/S004445102406e117

1. INTRODUCTION

For several decades, HgCdTe has remained one of the primary materials for infrared radiation detection [1]. The range of available wavelengths for commercial interband photodetectors based on HgCdTe extends from the near-IR range to approximately 25 μm, which is due to the wide possibilities for varying the bandgap of the solid solution. Since HgTe has virtually zero bandgap, working wavelengths beyond 25 μm are theoretically achievable in detectors based on HgCdTe solutions with high Hg content. However, several obstacles arise on the path to the far-IR range. Besides technological challenges, such as composition fluctuations or p-type doping problems for photodiodes, there are fundamental limitations on the material's detection capability related to carrier lifetime. As the bandgap decreases, the acceleration of non-radiative recombination processes leads to a reduction in carrier lifetime and corresponding decrease in sensitivity. Although this topic has been intensively studied for several decades, some quantitative uncertainties still remain, particularly regarding Auger recombination [2]. Another type of non-radiative processes – Shockley–Read–Hall (SRH) recombination is associated with defect/impurity centers that are always present in HgCdTe at least due to mercury vacancies. In HgCdTe, vacancy formation is essentially inevitable due to weak bonding Hg–Te, while their energy spectrum is still subject to debate [3–5]. Increasing mercury vacancy concentration through post-growth annealing is often used to convert HgCdTe films conductivity type from n-type to p-type. Carrier lifetimes during conversion typically decrease significantly [6], presumably because the emerging mercury vacancies serve as additional recombination centers. On the other hand, short carrier lifetimes enable the creation of high-speed IR detectors, including heterodyne type. Heterodyne receivers and mixers in the long-wavelength part of the

mid-IR range may be of interest for spectroscopy in astrophysics. In particular, studying emission spectra of cosmic objects, such as nebulae, at hydrogen characteristic lines (28.221 μm, 17.035 μm, 12.279 μm, 9.665 μm, 8.026 μm) allows visualization of heating and cooling of such objects, shock waves and collisions, and other effects [7].

Mercury vacancy is a double or two-charge acceptor. Such an acceptor can exist in three charge states: neutral A_2^0-center with two holes bound to it, singly ionized A_2^{-1}-center with one hole bound to it, and finally, fully ionized A_2^{-2}-center. Due to numerous studies, the spread of ionization energies known from literature for A_2^0 -center and A_2^{-1}-center is quite large. However, the existence of states located at 15–20 meV from the valence band edge has been reliably established [8–11]. Note that the difficulty in unambiguous determination of ionization energy in this case is also related to the fact that it overlaps with the energy of optical phonons, which in the solid solution are represented by HgTe-like and CdTe-like modes with energies from 15 to 17.5 meV and from 16 to 20 meV respectively. Thus, if the band gap in the material is from 30 to 40 meV (with Cd fraction in solid solution 18.8 %), one can expect that the discrete defect level appears near the middle of the band gap. During SRH recombination through mercury vacancies, the following recombination channels are possible:

• Through neutral vacancies (A_2^0-center). An electron is captured at the neutral center, forming A_2^{-1}-center. Then a hole is captured at this center (process 1: $A_2^0 + e = A_2^{-1}$, $A_2^{-1} + h = A_2^0$).

• Through A_2^{-1}-center. Either a hole is captured at the A_2^{-1}-center forming a neutral vacancy, and then an electron is captured at it (process 2: $A_2^{-1} + h = A_2^0$, $A_2^0 + e = A_2^{-1}$). Or an electron is captured at the A_2^{-1}-center forming A_2^{-2}-center, and then a hole is captured at this center (process 3: $A_2^{-1} + e = A_2^{-2}$, $A_2^{-2} + h = A_2^{-1}$).

• Through A_2^{-2}-center. A hole is captured at the fully ionized vacancy forming A_2^{-1}-center, then an electron is captured at this center (process 4: $A_2^{-2} + h = A_2^{-1}$, $A_2^{-1} + e = A_2^{-2}$).

Non-radiative capture of both holes and electrons occurs with the emission of optical and acoustic phonons. In all such processes, the law of energy conservation must be satisfied: the difference between the energy of the continuum state and the energy of the impurity-defect center state must be equal to the phonon energy. In this work, we focus on examining SRH recombination processes in a material with a bandgap from 35 to 40 meV. The wavelength range corresponding to these energies (from 30 to 35 μm) appears to be the next natural "frontier" for advancing HgCdTe-based detectors into the long-wavelength region. As a recombination center, we will consider the A_2^{-1}-center with an ionization energy of 20 meV, previously discovered in a series of studies on HgCdTe epitaxial layers grown by MBE method [12,13]. Thus, in the considered case, the capture of both holes and electrons into the state can occur with the emission of a single optical phonon. Comparison of calculation results with characteristic times for other recombination processes (Auger recombination and radiative recombination) shows that the considered type of SRH recombination can be the dominant channel for relaxation of non-equilibrium carrier concentration both at liquid helium temperature and at liquid nitrogen temperature.

2. CALCULATION METHOD

Below, we will calculate the capture times of holes to the states of the A_2^{-2}-center and electron capture times to the A_2^{-1}-center with emission of single optical phonons (processes 3,4). In the first case, the carrier must lose energy equal to the ionization energy of the A_2^{-1}-center (E_2), in the second case, the energy transferred to the phonon by the electron equals $E_g - E_2$, where E_g is the band gap width. As previously noted, the binding energy of the A_2^{-1}-center in narrow-band (up to 50 meV) HgCdTe layers is about 20 meV, and the band gap width changes rapidly depending on the composition of the solid solution. In the case of optical phonon emission, we will use Fermi's golden rule to calculate the intensity of carrier transitions from the valence band and conduction band to the ground state of the A_2^{-1}-center of the mercury vacancy. Due to lattice vibrations, a correction to the crystal potential ($\mathrm{d}V$), is introduced, which can be decomposed into two components: electrostatic macrofield ($\delta\overline{V}$) and deformation field ($\delta\widetilde{V}$): $\mathrm{d}V = \delta\widetilde{V} + \delta\overline{V}$ [14].The macrofield appears only in polar semiconductors, as polarization occurs due to the displacement of lattice atoms. In polar semiconductors, carriers interact with the macrofield much stronger than with the deformation potential [14], therefore in further

calculations only scattering on the macrofield (PO-mechanism) will be considered.

As known from [14], the probability of transverse optical phonon emission in this case equals zero. When considering the probability of longitudinal phonon emission per unit time in the case of a hole transition from the valence band or an electron from the conduction band to the ground state of the acceptor A_2^{-1}-center, it takes the form [14]

$$W_{if} = \int \left(\frac{16\pi^3 a^3}{m\omega_{LO}(q)}\right)\frac{e^2\gamma^2}{q^2} |\langle\Psi_{cont}| e^{iqr} |\Psi_0\rangle|^2 \cdot$$

$$\cdot (N_F(q)+1)\delta(\varepsilon_{cont} - m\omega_{LO}(q) - \varepsilon_0)d^3q, \quad (1)$$

where i and f are the initial and final states respectively, $N_F(q)$ are the occupation numbers of phonon states, $m = m_{Hg}m_{Te}/(m_{Hg}+m_{Te})$ — reduced mass of atoms in the elementary cell (tellurium and mercury atoms), q is the phonon wave vector, ω_{LO}), is the frequency of the longitudinal optical phonon (HgTe-like or CdTe-like), is the lattice constant of the solid solution $Hg_{1-x}Cd_xTe$, $\Psi_{cont,0}$, $\varepsilon_{cont,0}$ are the wave functions and energies of continuous spectrum states and the ground localized acceptor leve (A_2^{-2}-center of mercury vacancy). According to [14], the coefficient value for longitudinal optical phonons is presented as

$$\gamma = \sqrt{\frac{1}{4\pi}\left(\frac{1}{\varepsilon_\infty} - \frac{1}{\varepsilon_0}\right)\frac{m}{a^3}}\omega_{LO}(0), \quad (2)$$

where $\varepsilon_{\infty,0}$ — high-frequency and static dielectric permittivities of the HgCdTe solid solution respectively, $\omega_{LO}(0)$ is the frequency of the longitudinal optical phonon at $q = 0$. Values for HgTe and CdTe from [15] were used to obtain dielectric permittivity values for the solid solution by linear interpolation. According to [16], $\omega_{LO}(0) = 4.85\times10^{12}$ Hz and 4.24×10^{12} Hz for CdTe-like and HgTe-like phonons respectively. The energies and envelope wave functions of holes were obtained by solving the Schrödinger equation, which included the Kane Hamiltonian, acceptor ion potential, and central cell potential describing the chemical shift. This method is described in detail in [13]. The wave functions of continuous spectrum hole states were calculated beyond the Born approximation taking into account the impurity center potential [13], and the electron wave functions in the conduction band were chosen as plane waves.

Integrating expression (1) over the states of the continuous spectrum in the valence band/conduction band, taking into account the distribution function of holes/electrons, one can obtain the capture frequency of a particle (inverse capture time) from the continuous spectrum:

$$\frac{1}{\tau} = \sum_{cont} W_{cont\to f} f_{p,n}. \quad (3)$$

Paper [17] shows that the lifetime of piezo-acoustic electron scattering in the conduction band in HgCdTe layers is a fraction of picoseconds. Therefore, the distribution functions $f_{p,n}$ can be considered quasi-equilibrium:

$$f_{p,n} = \frac{1}{1+\exp\left(\frac{\varepsilon_{cont} - F_{p,n}}{T}\right)}, \quad (4)$$

where $F_{p,n}$ is the quasi-Fermi level for holes and electrons respectively ε_{cont} is the particle energy in the continuum of the conduction band or valence band.

The position of the quasi-Fermi level for holes is determined depending on the concentration of holes in the valence band and temperature according to expression [18]

$$p = \frac{2}{(2\pi)^3}\int\left(1+\exp\frac{-E_V + \frac{n^2k^2}{2m_{hh}} + F_p}{T}\right)^{-1} d^3k +$$

$$+\frac{2}{(2\pi)^3}\int\left(1+\exp\frac{-E_V + \frac{n^2k^2}{2m_{lh}} + F_p}{T}\right)^{-1} d^3k. \quad (5)$$

Here m_{hh} and m_{lh} are the effective masses of heavy and light holes in HgCdTe solid solution respectively, E_V is the energy of the valence band ceiling, T is temperature in energy units. Note that the mass of light holes is an order of magnitude less than the mass of heavy holes, therefore the second term in expression (2) is much smaller than the first and can be neglected. The calculated position of the

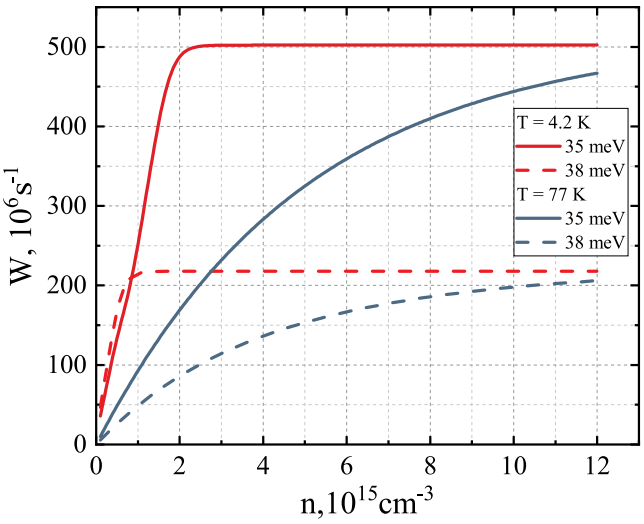

Fig. 1. Calculated frequencies of electron transitions from the conduction band to A_2^{-1}-center depending on their concentration at different values of HgCdTe bandgap The calculation was performed for concentration range from 10^{13} cm^{-3} to $1.2 \cdot 10^{16}$ cm^{-3}.

Fermi level was used in calculating the frequency of hole capture from the valence band according to expression (3).

The position of the quasi-Fermi level for electrons is determined depending on the concentration of electrons in the conduction band according to expression [18]

$$n = \frac{2}{(2\pi)^3}\int\left(1+\exp\frac{E_c+\frac{n^2k^2}{2m_e}-F_e}{T}\right)^{-1} d^3k. \quad (6)$$

Here m_e is the effective mass of electrons in the solid solution E_c is the energy of the conduction band bottom of HgCdTe.

For analyzing the obtained results in relation to real structures produced by MBE method [19], besides the carrier lifetime in the considered SRH process, it is necessary to determine the characteristic times of other processes: interband recombination during radiative transitions, as well as Auger processes. The radiative and Auger recombination times in this work were calculated using widely cited approximate analytical formulas, presented, for example, in works [2,20]. The expression for Auger recombination time includes, besides material constants, the threshold energy (E_{th}) of various Auger processes and parameter $|F1F2|^2$. In this work, the threshold energies were calculated not approximately (analytically), but numerically based on the energy spectrum obtained in the Burt-Foreman model with Kane Hamiltonian 8 × 8 [21, 21]. $F1$ and $F2$ represent the overlap integrals of wave functions in different states occupied by electrons during the Auger process. Analytical expression for $F1$ and $F2$ can be found in the classical work of Beattie and Landsberg [23], however, in the vast majority of works, the value $|F1F2|^2$ is considered as a fitting parameter [24]. Typically, in most publications $|F1F2| \sim 0.2$, however, in recent works, values around 0.05 are encountered. To account for data from various publications in analyzing the results of this work, below are provided Auger recombination times for $|F1F2|^2$ values across the entire range from 0.05 to 0.2.

3. RESULTS AND DISCUSSION

The frequencies of electron capture from the conduction band to A_2^{-1}-centers with emission of single optical phonons were calculated. Note that unlike the process of hole capture at acceptor levels, electron capture can only occur directly to the main acceptor level, since there are no intermediate levels between the conduction band and the main acceptor state. The calculation of electron capture frequency from the conduction band was performed for the main level of A_2^{-1}-center, located 20 meV above the valence band edge. Since the optical phonon energies range from 15 to 17.5 meV for HgTe-like phonon and from 18 to 20 meV for CdTe-like phonon, electron transitions to the ground state of A_2^{-1}-center will occur if the bandgap E_g is within the range of 35 to 40 meV.

Fig. 1 shows the calculated transition frequencies from the conduction band to the A_2^{-1}-center depending on the electron concentration in the band at different values of E_g and temperature T. It can be seen that with an increase in concentration from 10^{13} cm^{-3} there is a linear growth in transition intensity, which reaches saturation above a certain carrier concentration in the conduction band. This is due to the fact that transitions to acceptor states are possible only for carriers having kinetic energy within a certain range. For a band gap of 38 meV, it is no more than 20–18 = 2 meV (the difference between the maximum energy of the optical phonon and the energy gap between the conduction band edge and the acceptor level), and for a band gap of 35 meV, no more than 20–15 = 5 meV. With

increasing concentration, the transition frequency initially grows due to the increase in the number of particles emitting phonons, and then, when the Fermi level becomes higher than the band edge by more than 2 (5) meV and the number of particles participating in transitions becomes constant, the growth of transition frequency stops. At liquid nitrogen temperature, the dependence of transition frequency on carrier concentration in the band is smoother due to the smearing of the electron distribution function in the conduction band at elevated temperatures. It can be seen that the optical phonon emission time during electron capture at the A_2^{-1}-center for sufficiently high carrier concentration in the band is on the order of ns.

The frequencies of hole transitions from the valence band with optical phonon emission to the ground state of the A_2^{-2} mercury vacancy center were also calculated. It was found that the time of such transiti on for the solid solution with 18.8% cadmium content and bandgap of 36 meV (where the ionization energy of the A_2^{-2}-center is 18 meV) is 3 ps. Thus, the electron capture time for the A_2^{-1} mercury vacancy center was three orders of magnitude longer than the hole capture time. Therefore, it can be expected that the SRH recombination time is determined by electron transitions. In this case, the SRH recombination time can be calculated using the following formula (see Appendix)

$$t_{SRH} = t_{ph}\left(\frac{n}{N_{A_2^{-1}}}\right). \quad (7)$$

Here t_{SRH} is the relaxation time of electrons in the conduction band, t_{ph} is the phonon emission time during capture at one center, $N_{A_2^{-1}}$ concentration of A_2^{-1}-centers, n – electron concentration. Thus, to calculate the SRH recombination time in narrow-gap HgCdTe layers, it is necessary to know not only the phonon emission time but also the number of carrier capture centers, i.e., the number of A_2^{-1}-centers. The number of such centers is the sum of the equilibrium number of A_2^{-1}-centers. The number of such centers is the sum of the equilibrium number of A_2^{-1}-centers ($N^P_{A_2^{-1}}$) and the number of centers generated by excitation radiation ($N^G_{A_2^{-1}}$):

$$N_{A_2^{-1}} = N^P_{A_2^{-1}} + N^G_{A_2^{-1}}.$$

Considering that the process of hole capture at mercury vacancies is three orders of magnitude faster than electron capture at such centers, it can be assumed that when considering electron relaxation processes, the stationary distribution of holes across states has already been established.

Let's consider the following cases.

3.1. Material of *n* type

In this case, at low temperature, all mercury vacancies are in the charge state A_2^{-2} (acceptor centers are free of holes). A_2^{-1}-centers arise due to the capture of holes generated by exciting radiation ($N_{A_2^{-1}} = N^G_{A_2^{-1}}$). Their concentration equals the concentration of non-equilibrium holes (Δp), if the number of such holes does not exceed the number of mercury vacancies; otherwise, the holes will completely fill A_2^{-2}-centers (forming A_2^{-1}-centers), and the remaining particles will fill the emerging A_2^{-1}-centers, forming neutral mercury vacancies. Thus, in the case of HgCdTe — n-type material — the relation $N_{A_2^{-1}} \le \Delta p$. is valid. Since during optical excitation, the number of non-equilibrium holes equals the number of non-equilibrium electrons (Δn) for the SRH recombination time from relation (7) we have

$$t_{SRH} \ge t_{ph}\left(\frac{n}{\sqrt{\Delta n}}\right). \quad (8)$$

The equality in relation (8) is realized when the number of mercury vacancies exceeds the number of generated holes, i.e., in the case of low excitation intensity. In *n*-type material, the lifetime of non-equilibrium carriers in the SRH recombination process depends on their concentration, even when the latter is less than the dark concentration of electrons. This can lead to substantially non-exponential relaxation dynamics of excess carrier concentration, which complicates the analysis of experimental curves. Since the number of A_2^{-1}-centers is less than the total number of mercury vacancies, the following relation can be used to estimate the minimum SRH recombination time from expression (7):

$$t_{SRH} \ge t_{ph}\left(\frac{n}{N_{A_2}}\right). \quad (9)$$

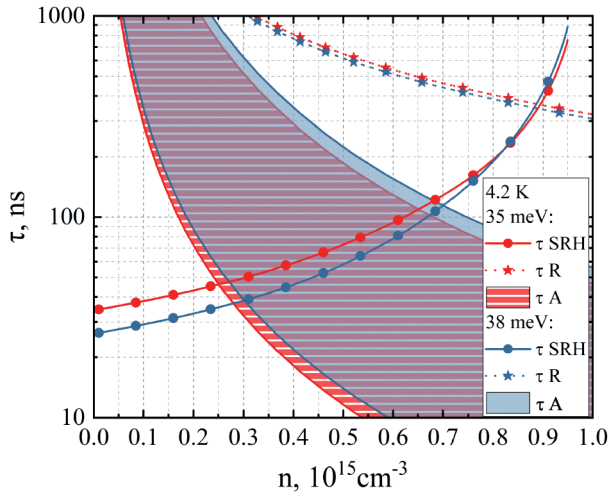

Fig. 2. Calculated for $T = 4.2$ K recombination times in p-type HgCdTe depending on the concentration of free electrons in the conduction band. The concentration of compensating donors equals 10^{15} cm^{-3}

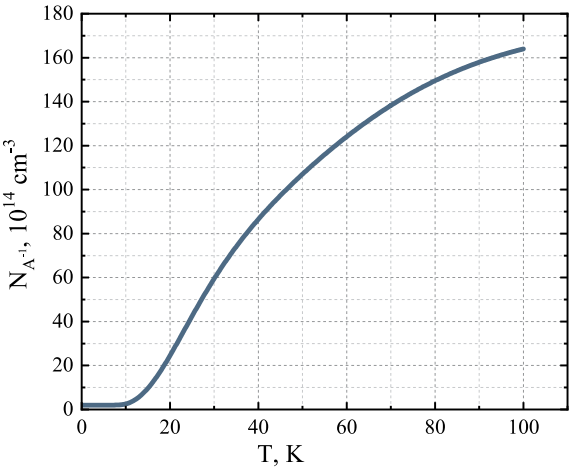

Fig. 3. Temperature dependence of the equilibrium concentration of A_2^{-1}-centers of mercury vacancies in the HgCdTe layer with Cd fraction in solution $x = 17.7$ %. The concentration of compensating donors is $N_D = 2 \cdot 10^{14}$ cm^{-3}, mercury vacancy concentration $N_A = 2.5 \cdot 10^{16}$ cm^{-3}

The equality in expression (9) is realized when the number of holes arising during pumping equals the number of double acceptors. At $T = 4.2$ K, the estimation of SRH recombination time from (9) for HgCdTe with a band gap of 35 meV gives a value of about 170 ns for an equilibrium electron concentration of $2 \cdot 10^{14}$ cm^{-3} and mercury vacancy concentration of $2 \cdot 10^{13}$ cm^{-3}, which satisfactorily agrees with experimental data [25]. At $T = 77$ K, the estimated SRH recombination times exceed 500 ns and thus do not contribute significantly to the total recombination time, since Auger recombination times are considerably shorter.

3.2. p-type material at T = 4,2 K

The equilibrium number of A_2^{-1}-centers at low temperature is determined by the degree of compensation: the number of such centers equals the number of compensating donors (N_D). Under illumination, as previously noted, the generated holes transition to A_2^{-1}-centers within about 3 ps, converting them into neutral A_2^0-centers. Then the number of A_2^{-1}-centers under illumination:

$$N_{A_2^{-1}} = N_d - \Delta p \tag{10}$$

Then, considering that $\Delta p = \Delta n$ and the concentration of equilibrium electrons at low temperature is negligibly small, expression (7) in this case takes the form

$$\tau_{SRH} = \tau_{ph}\left(\frac{N_d}{N_d - \Delta n}\right). \tag{11}$$

Figure 2 shows the graphs of carrier lifetime dependencies for three recombination processes (SRH recombination (τ_{SRH}) calculated from (10), radiative recombination (τ_R) and Auger recombination (τ_A)) on the concentration of free electrons in the conduction band at (10), on the concentration of free electrons in the conduction band at $T = 4.2$ K. Calculations were performed for HgCdTe p-type layer, corresponding to $E_g = 35$ meV and Eg = 38 meV. The concentration of compensating donors N_D is chosen to be 10^{15} cm^{-3}.

Mercury vacancy concentration is assumed to be $N_A > N_D$. For Auger recombination time τ_A the range of values is shown, corresponding to the variation of the fitting parameter $|F1F2|$ within the range from 0.05 to 0.2, similar to work [2]. Considering that the total relaxation time τ is defined as

$$\tau^{-1} = \tau_R^{-1} + \tau_{SRH}^{-1} + \tau_A^{-1}, \tag{12}$$

it corresponds to the shortest recombination time. Figure 2 shows that SRH recombination time will have a noticeable effect on in p-type material at free electron concentration (sum of equilibrium and non-equilibrium concentration) in the conduction band up to values of about $2 \cdot 10^{14}$ cm^{-3} or about

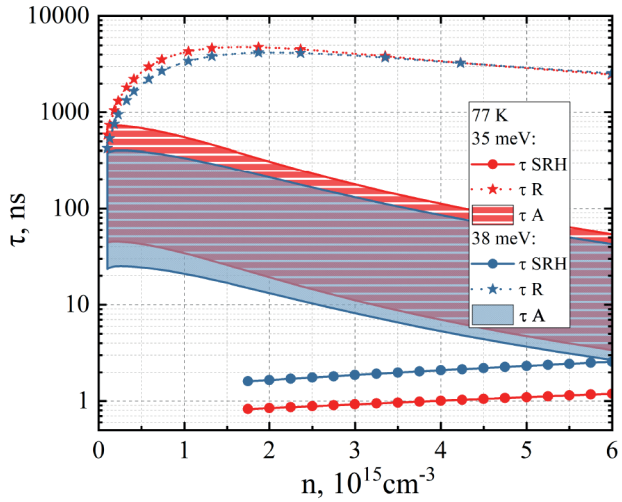

Fig. 4. Calculated for $T = 77$ K recombination times in HgCdTe p-type depending on the concentration of free electrons in the conduction band. The concentration of compensating donors is $N_D = 2 \cdot 10^{14}$ cm^{-3}, mercury vacancy concentration $N_A = 2.5 \cdot 10^{16}$ cm^{-3}

$6 \cdot 10^{14}$ cm^{-3} depending on the value of $|F1F2|^2$. At higher concentrations of non-equilibrium electrons, the total recombination time is controlled by Auger processes.

3.3 Material of p-type at $T = 77$ K

Fig. 3 shows the temperature dependence of the equilibrium concentration of A_2^{-1}-centers in the HgCdTe layer with Cd fraction in solution $x = 17.7$ %. The dependence was calculated using the method presented in work [26]. Mercury vacancy concentration $N_A = 2.5 \cdot 10^{16}$ cm^{-3} was chosen at the level of maximum achievable for low-temperature annealing of HgCdTe [27]. At $T = 77$ K the equilibrium concentration of free electrons in the conduction band was $1.75 \cdot 10^{15}$ cm^{-3}, which corresponds to typical "dark" concentration in epitaxial films grown by MBE method [19].

In Fig. 3, it can be seen that the concentration be noted that the band gap in the film with $N_{A_2^{-1}}$ at $T = 77$ K is $1.4 \cdot 10^{16}$ cm^{-3}. It should be noted that the band gap in the film with $x = 17.7$ % at $T = 77$ K is about 38 meV.

Fig. 4 shows a graph of carrier lifetime dependence for three recombination processes in HgCdTe p-type material with $E_g = 35$ meV and $E_g = 38$ meV. It can be seen that the SRH recombination time is on the order of several nanoseconds over a wide range of total electron concentrations in the conduction band and determines the overall lifetime. When the non-equilibrium electron concentration increases above $6 \cdot 10^{15}$ cm^{-3} , the expression for SRH recombination time without accounting for the change in mercury vacancy occupancy by non- equilibrium holes becomes inapplicable. Note that for concentrations near equilibrium, SRH recombination will remain the dominant process even with a tenfold decrease in mercury vacancy concentration. At the same time, it is known that during high-temperature annealing, it is possible to increase the vacancy concentration up to values of approximately $3 \cdot 10^{18}$ cm^{-3} [28], which theoretically allows reducing SRH recombination times to approximately 10 ps. The latter is of interest for heterodyne receivers, where ensuring effective mixing imposes rather strict requirements on mixer speed

4. CONCLUSION

In this work, electron and hole capture times for states of partially ionized mercury vacancy in HgCdTe solid solutions with a band gap of about 40 meV were calculated for different values of temperature and carrier concentration in bands. It is shown that electron transition times to vacancy states from the conduction band exceed the characteristic hole capture time by at least three orders of magnitude. Thus, the SRH recombination time is determined by the electron capture time to acceptor states. Comparison of rates of different recombination mechanisms shows that the SRH process determines the overall carrier lifetime in HgCdTe p-type with mercury vacancy concentration more than approximately $2 \cdot 10^{15}$ cm^{-3} both at liquid helium temperature and at liquid nitrogen temperature. The obtained results create prerequisites for controlling the photoresponse time in such materials, including in the sub-nanosecond range, by changing the concentration of mercury vacancies.

ACKNOWLEDGMENTS

The authors thank E.V. Andronov for help in developing the software used in this work.

FUNDING

This work was supported by grants from the Russian Science Foundation 22-12-00298 (calculation of electron and hole capture times for an isolated acceptor center) and the Russian Foundation for Basic Research 21-52-12020 (calculations of carrier lifetimes for various recombination processes).

APPENDIX

The number of electron captures by one acceptor center equals τ_{ph}^{-1}, then the change in the number of electrons (n) in the conduction band per unit time has the form

$$\frac{dn}{dt} = -\frac{1}{\tau_{ph}} N_{A_2^{-1}}, \tag{13}$$

here $N_{A_2^{-1}}$ — number of electron capture centers (A_2^{-1}-centers).

Formula (13) can be reduced to the form

$$\frac{dn}{dt} = -\frac{1}{\tau_{SRH}} n, \tag{14}$$

$$\frac{dn}{dt} = -\frac{N_{A_2^{-1}}}{n\tau_{ph}} n. \tag{15}$$

We obtain

$$\tau_{SRH} = \tau_{ph}\left(\frac{n}{N_{A_2^{-1}}}\right). \tag{16}$$

REFERENCES

1. W. Lei, J. Antoszewski, and L. Faraone, Appl. Phys. Rev. 2, 041303 (2015).
2. K. Jóźwikowski, M. Kopytko, and A. Rogalski, J. Appl. Phys. 112, 033718 (2012).
3. F. Gemain, I.C. Robin, M. De Vita et al., Appl. Phys. Lett. 98, 131901 (2011).
4. B. Li, Y. Gui, Z. Chen et al., Appl. Phys. Lett. 73, 1538 (1998).
5. T. Sasaki, N. Oda, M. Kawano et al., J. Crystal Growth. 117, 222 (1992).
6. V. V. Rumyantsev, M. A. Fadeev, S. V. Morozov et al., Semiconductors 50, 1679 (2016).
7. M. G. Wolfire and A. Konigl, The Astrophys. J. 383, 205 (1991).
8. K. D. Mynbaev, A. V. Shilyaev, N. L. Bazhenov et al., Semiconductors. 49, 367 (2015).
9. F. Gemain, I. C. Robin, S. Brochen et al., J. Electr. Materials. 41, 2867 (2012).
10. X. Zhang, J. Shao, L. Chen et al., J. Appl. Phys. 110, 043503 (2011).
11. X. Chen, M. Wang, L. Zhu et al., Appl. Phys. Lett. 123 (2023).
12. A. Ikonnikov, V. Rumyantsev, M. Sotnichuk et al., Semiconductor Science and Technology 38, 085003 (2023).
13. V. V. Rumyantsev, D. V. Kozlov, S. V. Morozov et al., Semiconductor Science and Technology 32, 095007 (2017).
14. V. F. Gantmakher, I. B. Levinson, Carrier Scattering in Metals and Semiconductors, Nauka, Moscow (1984).
15. O. Madelung, Semiconductors: Data Handbook, Springer-Verlag, New York (2003).
16. D. N. Talwar and M. Vandevyver, J. Appl. Phys. 56, 1601 (1984).
17. D. V. Kozlov, M. S. Zholudev, K. A. Mazhukina et al., Semiconductors Physics and Technology (2023).
18. V. L. Bonch-Bruevich, S. G. Kalashnikov, Physics of Semiconductors, Nauka, Moscow (1977).
19. S. Krishnamurthy, M. A. Berding, and Z. G. Yu, J. Electron. Materials 35, 1369 (2006).
20. E. G. Novik, A. Pfeuffer-Jeschke, T. Jungwirth et al., Phys. Rev. B 72, 035321 (2005).
21. S. V. Morozov, V. V. Rumyantsev, M. S. Zholudev et al., ACS Photonics 8, 3526 (2021).
22. A. R. Beattie and P. T. Landsberg, Proc. of the Royal Society A: Mathematical, Physical and Engineering Sciences 249, 16 (1959).
23. A. R. Beattie and P. T. Landsberg, Proc. of the Royal Society A: Mathematical, Physical and Engineering Sciences 249, 16 (1959).
24. N. L. Bazhenov, K. D. Mynbaev, G. G. Zegrya, Semiconductors Physics and Technology 49,444 (2015).
25. V. V. Rumyantsev, S. V. Morozov, A. V. Antonov et al., Semiconductor Science and Technology 28, 125007 (2013).
26. D. V. Kozlov, M. S. Zholudev, V. V. Rumyantsev et al., Semiconductors Physics and Technology 56, 465 (2022).
27. P. A. Bakhtin, S. A. Dvoretsky, V. S. Varavin et al., Semiconductors Physics and Technology 38, 1207 (2004).
28. D. Chandra, H. F. Schaake, J. H. Tregilgas et al., J. Electronic Materials 29, 729731 (2000).